Linear augmented-Slater-type-orbital method for electronic-structure calculations. V. Spin-orbit splitting in Cu_3Au

J. W. Davenport, R. E. Watson, and M. Weinert
Department of Physics, Brookhaven National Laboratory, Upton, New York 11973-5000
(Received 23 December 1987)

We have used local-density-functional theory to calculate the energy bands, heat of formation, and core-level shift in the classic ordering alloy Cu_3Au. Contrary to expectations we find that the d bands are largely nonoverlapping with the gold region extending from -4 to -7 eV relative to the Fermi level. The copper d levels are concentrated in the range -1 to -4 eV. Addition of spin-orbit splitting strongly mixes the gold states, producing features which are predominantly $j=\frac{5}{2}$ and $j=\frac{3}{2}$ with the $\frac{5}{2}$ level split weakly by the residual crystal-field effects. This agrees with the interpretation of photoemission data by Eberhardt *et al.* The total energy yields a heat of formation of -0.048 eV/atom compared with the experimental value of -0.07 eV/atom. The Au $4f$ core-level position was calculated using a total-energy approach. The fully relaxed shift was found to be 0.3 eV (to larger binding energy) compared with the experimental value of 0.48 eV. The absolute value of the core-level binding energy was calculated to be 84.1 eV, compared to 84.40 eV experimentally.

I. INTRODUCTION

The copper-gold system is one of the most interesting alloy systems for study. It is a classical example of an order-disorder transition[1] and shows a whole range of long-period structures.[2] It has motivated a large body of work on the Ising antiferromagnet, to which it is equivalent.[3-5] In addition, its surface properties have recently been investigated[6-8] and photoemission spectroscopy[9-13] has been done on the valence and $4f$ core levels.

Despite this there have been relatively few self-consistent calculations of the electronic structure of the copper-gold system.[14-16] A non-self-consistent calculation by Skriver and Lengkeek has explored the energy bands.[17] Stimulated by recent photoemission work, we have calculated the heat of formation, energy bands, and core-level shift of one member of this series Cu_3Au.

The crystal structure is cubic and may be obtained from fcc copper by replacing each of the atoms at the cube corners by gold with the atoms at the face centers remaining copper.

The plan of this paper is as follows: In Sec. II we describe the calculational techniques, in Sec. III we discuss the total energy and heat of formation, in Sec. IV the energy bands including the density of states and spin-orbit splitting, and in Sec. V the core-level shift. Section VI contains a summary and in the Appendix we describe the calculation of the spin-orbit splitting.

II. CALCULATIONS

We have used the density-functional theory to calculate the energy bands and total energies of fcc, Cu, Au, and Cu_3Au. To solve the density-functional equations, we have used the recently developed linear augmented-Slater-type-orbital method.[18,19] In this method we utilize a Bloch sum of Slater-type orbitals (STO's) to span the space between nonoverlapping spheres centered on each atom. Then,

$$\psi_{inlm}(\mathbf{r})=\frac{1}{(N_c)^{1/2}}\sum_s \exp(i\mathbf{k}\cdot\mathbf{R}_s)\phi_{nlm}(\mathbf{r}-\mathbf{R}_s-\tau_i)\ , \quad (1)$$

where the sum s extends over all the cells of the system and ϕ is a Slater-type orbital,

$$\phi_{nlm}(\mathbf{r})=A_{nl}r^{n-1}e^{-\zeta r}Y_{lm}(\hat{\mathbf{r}})\ . \quad (2)$$

In Eq. (2), A is the normalization constant. To span the space inside the spheres, the Bloch sum is matched onto numerical solutions of the spin-orbit-less Dirac equation (see Appendix). As in other linear methods,[20] we use the functions $g(r)$ and their energy derivatives $\dot{g}(r)$ so that inside the jth sphere

$$\psi_{inlm}(\mathbf{r})=\frac{1}{(N_c)^{1/2}}\sum_\Lambda [\beta_{N,j\Lambda}g_\lambda(r_j) + \alpha_{N,j\Lambda}\dot{g}_\lambda(r_j)]Y_\Lambda(\hat{\mathbf{r}})\ , \quad (3)$$

where N is a composite index giving (i,n,l,m) and Λ is a composite index giving (λ,μ). The sum in Eq. (3) was extended to $\lambda\leq 8$. Actually, it is much more convenient to use the reciprocal-lattice representation of Eq. (1),

$$\psi_{inlm}(\mathbf{r})=\frac{1}{(N_c)^{1/2}}\sum_s \exp[i(\mathbf{k}+\mathbf{g}_s)\cdot(\mathbf{r}-\tau_i)] \times\frac{1}{\Omega}\tilde{\phi}_{nlm}(\mathbf{k}+\mathbf{g}_s)\ , \quad (4)$$

where Ω is the unit-cell volume, $\mathbf{g}_s$ is a reciprocal-lattice vector, and $\tilde{\phi}_{nlm}$ is the Fourier transform of ϕ. The Fourier transform of a STO is known analytically.[18]

In our calculations the ζ's were chosen to minimize the total energy of the metallic element. Our ζ values for

copper and gold are given in Table I.

In all cases we used the experimental lattice constants given in Table I. The sphere sizes (also in Table I) were chosen to be touching in the compound. When computing the heat of formation, we used the total energy of the metallic elements obtained with the same sphere radii. These radii were slightly smaller than the touching sphere radii (defined by the elemental metals).

The density and total energy were obtained by sampling the Brillouin zone at a relatively small number of special points. In such a procedure it is important to broaden the levels slightly; we use a broadening function

$$\gamma(\varepsilon-\varepsilon_0)=\frac{1}{4k_BT}\mathrm{sech}^2\left[\frac{\varepsilon-\varepsilon_0}{2k_BT}\right] \tag{5}$$

because its integral is the Fermi-Dirac distribution function. For these calculations we used $k_BT=0.001$ hartree (1 hartree=27.212 eV). The potential is sphere and volume averaged to a muffin-tin form. This should be a good approximation for such a close-packed system.

In using the reciprocal-lattice representation, Eq. (4), all reciprocal-lattice vectors with $|\mathbf{g}_s| \le g_{\mathrm{cut}}$ were included. For copper and gold we took $g_{\mathrm{cut}}=8\pi/a$. This corresponds to 65 reciprocal-lattice vectors at the center of the Brillouin zone for Cu or Au; or, since the radius of touching spheres in the fcc lattice is $R_s=a/2\sqrt{2}$, it corresponds to $R_s g_{\mathrm{cut}}=8.89$. For Cu_3Au, $g_{\mathrm{cut}}=8\pi/a$ yields 256 reciprocal-lattice vectors at the zone center. Another way of characterizing the cutoff is to give the energy of a plane wave with wave vector g_{cut}. This is $\hbar^2 g_{\mathrm{cut}}^2/2m$ or 6.79 hartree for Cu.

As we have indicated previously,[21] the (reciprocal-) lattice sums are not completely converged with such values of g_{cut}. In fact, the total energy passes through a shallow minimum at $g_{\mathrm{cut}}=8\pi/a$. To be sure that we indeed have found the correct value for the heat of formation, we extended the basis set by adding a second set of s, p, and d functions (leading to a 72×72 secular matrix for Cu_3Au).

TABLE I. Parameters used in the calculations.

ζ (units of a_0^{-1})	($a_0\cong0.529$ Å)			
Cu	3*d*	1.72	4*d*	2.22
	4*s*	0.68	5*s*	1.85
	4*p*	1.37	5*p*	2.22
Au	5*d*	2.50	6*d*	2.66
	6*s*	2.70	7*s*	2.32
	6*p*	2.00	7*p*	2.66

Lattice constants	(units of a_0)
Cu	6.831
Au	7.707
Cu_3Au	7.070

Sphere sizes	(units of a_0)
Cu	2.348
Au	2.649

TABLE II. Cohesive energies (in eV). ($4k$) implies four special points in the Brillouin-zone sums for Cu_3Au and ten points for Cu and Au. ($10k$) implies ten points for Cu_3Au and 28 points for Cu and Au.

	1ζ ($4k$)	1ζ ($10k$)	2ζ ($4k$)	Expt.
Cu	−3.865	−3.907	−4.137	−3.49
Au	−3.355	−3.406	−3.444	−3.81
Cu_3Au	−15.094	−15.273	−16.048	−14.58
ΔH	−0.144	−0.146	−0.193	−0.297
$\Delta H/4$	−0.036	−0.037	−0.048	−0.074

With these "double-ζ" basis sets, no such minimum is observed and the heat of formation is changed by only 0.01 eV/atom (from −0.036 to −0.048 eV/atom; experiment is −0.074 eV/atom).

In our calculations the core levels are not frozen, but are recalculated in each iteration. However, they are treated as atoms in a potential given by the spherical potential inside the spheres and by the constant (muffin-tin zero) at large radii. The core charge which is outside the muffin-tin radius is simply added to the interstitial density.

Finally, we have used the Hedin-Lundqvist[22] form for the correlation energy.

III. TOTAL ENERGY

The total energy of the various metals is quite large owing to the large contribution from the cores. It is more physical to think in terms of the valence energy, which we obtain by subtracting the energy of an ion with all the valence electrons removed. This energy is roughly the same as what would be obtained in a pseudopotential[23] or frozen-core calculation,[24] except that it does not assume frozen cores in the solid and, therefore, is a quantity which can, in principle, be compared with experiments. For copper the energy of the ion with eleven electrons removed is −43 644.411 eV. The total energy of the copper atom is −44 961.324 eV and, therefore, the valence energy is −1316.913 eV. For gold we find a valence energy of −907.058 eV. These calculations were spin restricted. To obtain the cohesive energies for copper and gold, it is necessary to add the spin-polarization energy that we have taken from other calculations. For copper the result of Janak, Moruzzi, and Williams[25] is −0.24 eV, while for gold Brooks and Johansson[26] give −0.12 eV. The cohesive energies are given in Table II.

IV. ENERGY BANDS

A. Density of states

An overview of the band structure of Cu_3Au has already been given by Skriver and Lengkeek.[17] Basically, one finds a broad s-p-band crossing and hybridizing with the d bands, just as occurs for pure copper and gold. The Fermi level lies above the d complex as in any noble metal. This is illustrated in Fig. 1, which shows the density

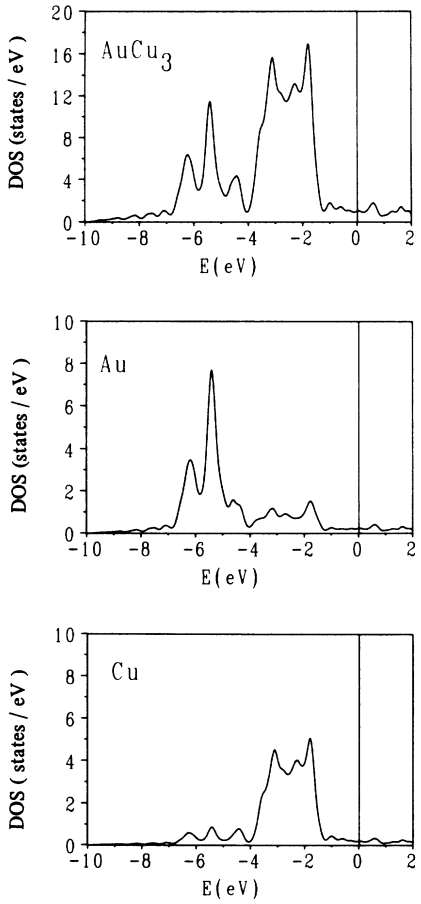

FIG. 1. Density of states (DOS) for Cu_3Au. The top panel is the total DOS, while the middle and lower panels are the partial densities for gold and copper, respectively. The partial DOS is defined by projection into the muffin-tin spheres.

of states for the compound as well as the projected densities of states in the gold and copper spheres. These state densities were obtained by calculating the energy bands at 35 points in the irreducible wedge of the Brillouin zone and then broadening each eigenvalue with a Gaussian with a full width at half maximum of 0.25 eV. The interesting feature of the projected state densities is that the gold states are very largely concentrated in a relatively narrow band between -4 and -7 eV with respect to the Fermi energy. This is somewhat surprising since copper and gold (being both noble metals) have been expected to form a single heavily hybridized d band. In fact, previous calculations[9,16,17] have also shown that the deeper states are predominantly of gold character. In a similar way it can be seen that the copper d band lies very largely in the range -1 to -4 eV.

For comparison, the density of states (DOS) for pure gold is shown in Fig. 2. It can be seen that the states extend from about -2 to -8 eV, which is quite different from Cu_3Au. We have also carried out a separate calculation on simple-cubic gold with a lattice constant equal to that of Cu_3Au. In this case the d-band DOS consists of a single peak with a full width at half maximum of

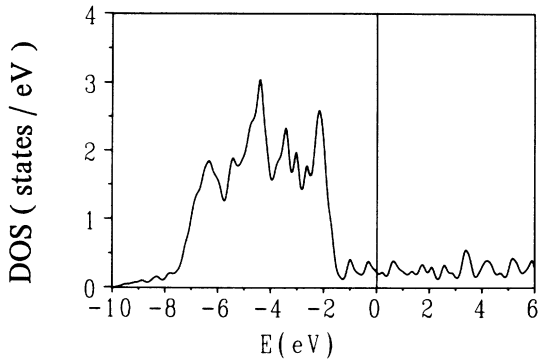

FIG. 2. Density of states for metallic gold.

~ 0.5 eV. This is close to the width of the peaks in the gold portion of the Cu_3Au spectrum (Fig. 1, middle panel). The fact that there are three such peaks is due to crystal-field splitting by the nearest-neighbor copper atoms.

B. Scalar-relativistic band structure along Γ-X

Our scalar-relativistic bands along the Δ line (i.e., along the z axis) from Γ to X are given in Fig. 3. For clarity only the bands of Δ_1 (s, p_z, d_{z^2}) and Δ_5 (p_x, p_y, d_{xz}, d_{yz}) symmetry are shown. This should be an aid to understanding photoemission data along the [001] direction since in the absence of spin-orbit splitting only states of these two symmetries contribute to normal photoemission. In the "gold region" near -6 eV there are also Δ_2 ($d_{x^2-y^2}$) and $\Delta_{2'}$ (d_{xy}) states which are nearly degenerate with the Δ_1 and Δ_5 states shown in the figure. Therefore, there is a complete set of Au d states in this energy range. The Mulliken population[27] for these states ranges from roughly 65% to 85% gold. If a state were uniformly distributed and using the Wigner-Seitz radius of pure gold (3.01 a.u.$=1.6$ Å), we find that the fraction of the unit-cell volume occupied by gold is $\sim 32\%$. Therefore, these states may be characterized as predominantly gold states, although there is a significant admixture of copper as well.

In Fig. 4 we compare the states at the zone center of Au and Cu_3Au. It can be seen that the ordering at Γ is reversed from that in pure gold (and other fcc metals). That is the Γ_{12} (e_g) level lies at higher binding energy than the $\Gamma_{25'}$ (t_{2g}) level. This is what would be observed for the splitting of a d level in a cubic crystal field or in a simple-cubic lattice and is further testimony to the essentially atomic character of these states.

Finally, we note that the states between 0 and -5 eV are described reasonably well by taking the bands of pure fcc copper and folding them at $k=\pi/a$, which corresponds to the zone boundary in Cu_3Au but is only halfway to the fcc zone boundary. This is further testimony that the bands in this energy range are essentially copper in nature.

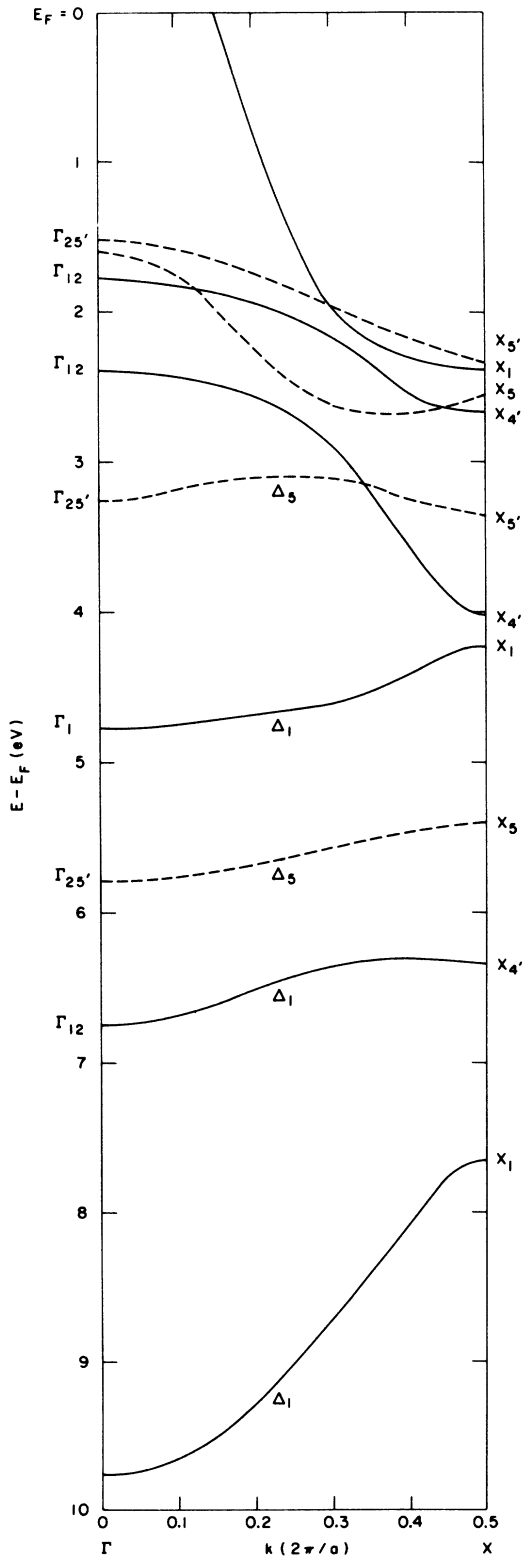

FIG. 3. Scalar-relativistic energy bands of Cu_3Au from Γ-X. The X point is at π/a. For clarity, only states of Δ_1 and Δ_5 symmetry are shown. The Δ_1 and Δ_5 states near -6 eV are predominantly of gold character, as discussed in the text. Also there is a goldlike Δ_2 state ($d_{x^2-y^2}$) nearly degenerate with the Δ_1 state near -7 eV, and a $\Delta_{2'}$ state (d_{xy}) nearly degenerate with the Δ_5 state near -6 eV.

C. Spin-orbit splitting

In atomic gold the experimental spin-orbit splitting of the d level is 1.50 eV. This is larger than the t_{2g}-e_g splitting for the "gold' states at the zone center of our scalar-relativistic calculation, which is 0.95 eV. Therefore, it is important to investigate the spin-orbit interaction for these bands. We have done this following McDonald, Pickett, and Koelling[28]—the details are in the Appendix.

The result is that the spin-orbit interaction can be obtained by starting from Eq. (3), multiplying by a spin function and forming the spin-orbit Hamiltonian

$$H_{\mathrm{SO}}=\left\langle \psi_{inlm}(\mathbf{r})\chi_s \left| \frac{1}{2M^2c^2}\frac{1}{r}\frac{dV}{dr}\mathbf{L}\cdot\mathbf{s} \right| \psi_{i'n'l'm'}\chi_s \right\rangle . \quad (6)$$

Here, L is the orbital and s the spin angular momentum. This doubles the size of the matrix to be diagonalized, but since our matrices are relatively small (36×36 for the single-ζ basis) it is not an undue expense. In evaluating Eq. (6) the contributions from the interstitial vanish because $dV/dr=0$ there. It is customary to define a spin-orbit–interaction parameter by

$$\xi_\lambda=\frac{\hbar^2}{2c^2}\int \frac{g_\lambda^2(r)}{M^2}\frac{1}{r}\frac{dV}{dr}r^2dr . \quad (7)$$

In an atom this completely specifies the splitting. However, in a solid it is more complicated because from Eq. (3), the basis functions contain energy derivatives of g and are summed over λ with $\mathbf{k}$-dependent coefficients β and α. For an isolated atom the spin-orbit splitting of the d level is $\frac{5}{2}\xi_d$. The calculated splitting in the atom is 1.61 eV, in reasonable agreement with experiment (1.50 eV). This implies $\xi_d=0.64$ eV. For Cu_3Au the calculated splitting parameters are 0.62 eV for gold and 0.11 eV for copper. Both of these within 0.02 eV of those calculated for the isolated atom.

As a test of our theory, we have calculated the splitting of the bands in fcc gold. The result at Γ is shown in Fig. 4 where it is compared with the result for Cu_3Au. The splittings are in good agreement with other relativistic calculations.[29]

The spin-orbit-split energy bands from Γ-X are shown in Fig. 5. They have been labeled according to the standard double-group notation.[30] In this figure we have shown all the bands because, as a result of the spin-orbit interaction, they all contribute to the normal photoemission. While the band structure has become more complicated, certain general features emerge. First, the range 0 to -5 eV is not perturbed nearly as much as the range -5 to -7 eV. This again reflects the fact that the states nearer the Fermi level are largely of copper origin and the spin-orbit effects are much less for copper than gold.

The states from -5 to -7 eV are strongly perturbed. In fact, the ordering at Γ reflects a "weak-crystal-field" situation[31] in which the atomic $d_{3/2}$ state shifts and carries a Γ_{8+} label and the $d_{5/2}$ state splits into Γ_{7+} and Γ_{8+}.

To illustrate the essential physics, we have considered a model Hamiltonian which consists of a crystal-field-split d level plus the spin-orbit interaction. The Hamil-

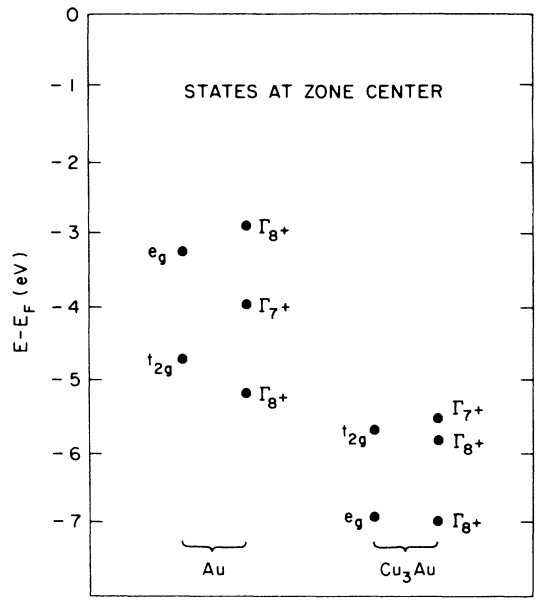

FIG. 4. States at the zone center for Au and Cu_3Au, both with and without spin-orbit splitting.

tonian is then a 10×10 matrix. However, using the following basis functions, it can be block-diagonalized into two 3×3 and two 2×2 matrices: for basis functions

$$(Y_{2,-2}\chi_\uparrow,\ Y_{2,2}\chi_\uparrow,\ Y_{2,-1}\chi_\downarrow)$$

or

$$(Y_{2,1}\chi_\uparrow,\ Y_{2,2}\chi_\downarrow,\ Y_{2,-2}\chi_\downarrow)\ ,$$

we have

$$H=\begin{bmatrix} -p-\xi & -5p & \xi \\ -5p & -p+\xi & 0 \\ \xi & 0 & 4p+\xi/2 \end{bmatrix},$$

and for basis functions

$$(Y_{2,0}\chi_\uparrow,\ Y_{2,1}\chi_\downarrow)$$

or

$$(Y_{2,-1}\chi_\uparrow,\ Y_{2,0}\chi_\downarrow)\ ,$$

we have

$$H=\begin{bmatrix} 4p-\xi/2 & (\sqrt{6}/2)\xi \\ (\sqrt{6}/2)\xi & -6p \end{bmatrix}.$$

Here the Y's are the usual spherical harmonics and the χ's are spin functions. p is the crystal-field-splitting parameter and ξ is the spin-orbit-splitting parameter.

This model spans the range from no spin orbit ($\xi=0$) to no crystal field ($p=0$). For $\xi=0$ we obtain a t_{2g} level at $4p$ and an e_g level at $-6p$. Fitting to our scalar-relativistic bands at Γ, we obtain $10p=0.95$ eV or $p=0.1$ eV. The other limit, $p=0$, yields a sixfold-degenerate level at ξ which is a $d_{5/2}$ atomic level and a fourfold level at $-\frac{3}{2}\xi$ which is a $d_{3/2}$ atomic level. Therefore, the atomic spin-orbit splitting is $\frac{5}{2}\xi$, and fitting to the isolated atom yields $\xi=0.62$ eV.

The behavior as a function of ξ for fixed $p=0.1$ eV is shown in Fig. 6. Examination of the eigenvectors shows that the Cu_3Au case, $\xi=0.62$ eV, is close to the atomic

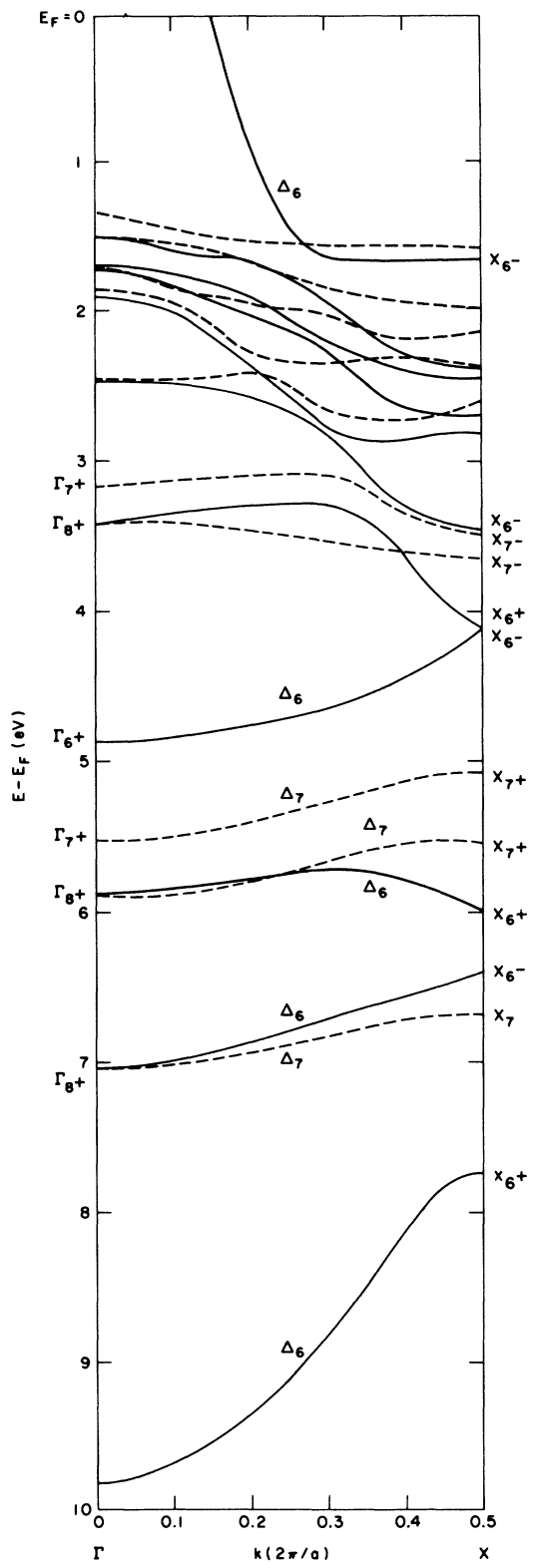

FIG. 5. Spin-orbit splitting of the energy bands for Cu_3Au from Γ-X.

limit. In fact, the state at -1.1 eV is 90% $j=\frac{3}{2}$, the state at 0.58 eV is 90% $j=\frac{5}{2}$, and the state at 1.1 eV is 100% $j=\frac{5}{2}$. Christensen[32] has described the spin-orbit splitting in fcc gold as a perturbation on the band splitting. He notes, however, that for slightly larger separation, the perturbation theory would break down. Here we see an example of this where it is best to treat both on an equal footing. The cohesive energy should not be sensitive to spin orbit because the bands which split are filled.

V. CORE-LEVEL SHIFT

We have also calculated the core-level binding energy for the gold $4f_{7/2}$ level. This is the energy required to take an electron from the $4f$ orbital up to the Fermi level. Our procedure involves a self-consistent calculation of the total energy of Cu_3Au with a core hole placed on every gold site. This assumes that the final-state relaxation, or screening, is sufficiently short ranged that these holes do not interact with each other. We have previously[33] tested this assumption by calculating the core-level binding energy of pure gold using the Cu_3Au crystal structure and placing the core hole at each cube corner. By extrapolating to infinite spacing, we showed that the error in such a calculation due to the proximity of adjacent holes is only 0.07 eV. In this way we find that the binding energy of the $4f_{7/2}$ level is 84.1 eV. The same-size supercell in pure gold (i.e., with the Cu_3Au structure) yields 83.8 eV. Therefore, the core-level shift is $+0.3$ eV. This compares with the experimental value of the shift, which is $+0.48$ eV (from 83.92 eV for bulk gold to 84.40 eV for Cu_3Au).

In previous work[33] we have shown how to partition this shift into an initial- and a final-state part by calculating the change in energy with a frozen charge density. In that work we found that for gold the initial-state shift between the atom and the solid was given accurately by the change in eigenvalue of the core level. We assume that the same is true here. The change in eigenvalue (relative to the Fermi level) between gold and Cu_3Au implies a change in binding energy of $+1.0$ eV for the single-ζ basis and $+0.8$ eV for the double-ζ basis. Since the fully relaxed change is only 0.3 eV, there is a differential relaxation of 0.5–0.7 eV between gold and Cu_3Au. That is to say, Cu_3Au has a larger relaxation energy than gold does.

Since gold is much more electronegative than copper, it might be thought that there would be charge transfer onto the gold, causing the core level to move to lower binding energy. However, it has been known for some time[34] that this can be explained as being due to compensating s and d charge transfer. There is, in fact, an increase in the s-like charge at the gold site. This is apparent in our calculations by examining the charge density near the nucleus and in experiments from the Mössbauer isomer shift. However, the site remains nearly neutral, implying a decrease in d-like charge which has a larger Coulomb interaction with the $4f$ levels and leads to the observed increase in binding energy. Similar results were found in our previous work on gold $5d$ alloys.[19]

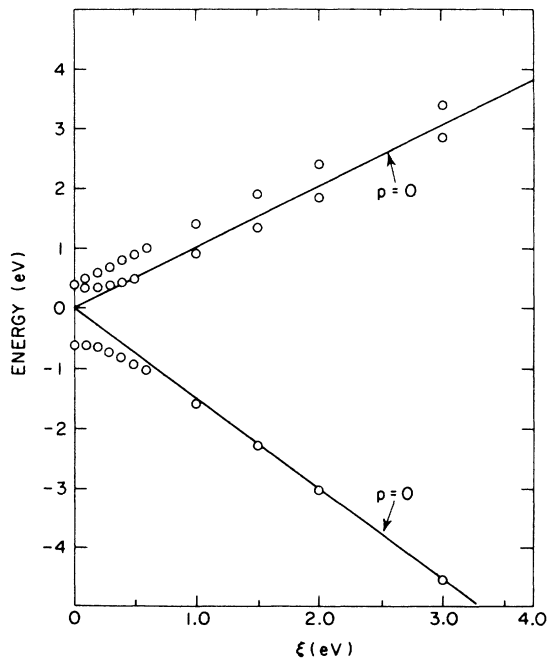

FIG. 6. Energy bands at zone center in Cu_3Au vs spin-orbit interaction parameter ξ. Levels obtained from the model Hamiltonian as described in the text.

VI. DISCUSSION

Copper and gold are both noble metals with $d^{10}s$ configurations in the atom. Therefore, one might expect that they would form a compound with a common heavily hybridized d band. DiCenzo and co-workers[11,12] have suggested that the density of states of Cu_3Au should, therefore, resemble a superposition of pure gold and pure copper densities of states. This is not the case. As was apparent from the calculations of Skriver and Lengkeek,[17] the band structure consists of distinct gold and copper $5d$ bands. We have illustrated this using self-consistent calculations of the electronic structure which are in somewhat better agreement with experimental photoemission studies.[10–12] Analysis of the bands using Mulliken populations, spin-orbit splitting, and projected densities of states all suggest the essentially "split-band" character of the states. In addition, we have calculated the heat of formation and Au $4f$ core-level shift and obtained good agreement with experiments.

Note added in proof. After submission of this paper, we became aware of similar calculations by G. K. Wertheim, L. F. Matheiss, and D. N. E. Buchanan (unpublished).

ACKNOWLEDGMENTS

This work was supported by the Division of Materials Sciences, U.S. Department of Energy, under Contract No. DE-AC02-76CH00016 and by a grant of computer time at the National Magnetic Fusion Energy Computing Center, Livermore, California.

APPENDIX: SPIN-ORBIT SPLITTING

We have generally followed Koelling and Harmon[35] in constructing a "spin-orbit-less" Dirac equation for the

valence states. The core states are treated fully relativistically. This leads to a second-order Hamiltonian for the radial function $g(r)$,

$$h_l(r)g_l(r)=\varepsilon g_l(r) , \tag{A1}$$

where

$$h_l(r)=-\frac{\hbar^2}{2M}\left[\frac{d^2}{dr^2}+\frac{2}{r}\frac{d}{dr}-\frac{l(l+1)}{r^2}\right] -\frac{\hbar^2}{4M^2c^2}\frac{dV}{dr}\frac{d}{dr}+V(r) . \tag{A2}$$

Here, $M=m[1+(\varepsilon-V)/2mc^2]$ and the other symbols have their usual meaning. We then form

$$\psi_A=g_l(r)Y_{lm}(\hat{\mathbf{r}})\chi_s , \tag{A3}$$

where Y_{lm} is a spherical harmonic and χ_s is a spin function. We take this to be a trial solution for the large component of the Dirac equation. A full trial solution would be

$$\psi=\begin{bmatrix}\psi_A\\ \psi_B\end{bmatrix} , \tag{A4}$$

where ψ_B is the small component. For a true Dirac spinor

$$\psi_B=\frac{1}{2Mc}\sigma\cdot\mathbf{p}\psi_A , \tag{A5}$$

where $\sigma\cdot\mathbf{p}=\sigma_x p_x+\sigma_y p_y+\sigma_z p_z$ and the σ's are the standard Pauli matrices. We have assumed here an isolated atom with a single (l,m) value. In the solid equation (A3) would be replaced by Eq. (3) multiplied by a spin function. However, to keep the algebra simple we will stay with the atom.

Using Eqs. (A3)–(A5) it is possible, though tedious, to construct the particle density

$$n(\mathbf{r})=\psi^\dagger\psi=g_l^2\mid Y_{lm}\mid^2+\frac{\hbar^2}{4M^2c^2}\left[\frac{\partial g}{\partial r}\right]^2\mid Y_{lm}\mid^2+\frac{\hbar^2}{4M^2c^2}g_l^2\frac{l(l+1)}{r^2}\mid Y_{lm}\mid^2-\frac{\hbar}{2M^2c^2}\frac{g(r)}{r}\frac{\partial g}{\partial r}\chi_s^\dagger Y_{lm}^*\sigma\cdot\mathbf{L}Y_{lm}\chi_s . \tag{A6}$$

At the suggestion of McDonald, Pickett, and Koelling, we have retained the first two terms in this expression to define the charge density. However, the last two are of the same order in $1/c^2$ and, as such, should be included. The last term would vanish for closed-shell systems and the third term would vanish for s states but might be important for p states.

The energy eigenvalues may also be calculated by explicitly evaluating the expectation value of the Dirac Hamiltonian:

$$H_D=c\boldsymbol{\alpha}\cdot\mathbf{p}+(\beta-1)mc^2+V , \tag{A7}$$

where $\boldsymbol{\alpha}$ and β are the usual 4×4 Dirac matrices and we have explicitly subtracted the rest energy of the electron. Then,

$$\langle\psi\mid H_D\mid\psi\rangle=\int(\psi_A^\dagger,\psi_B^\dagger)H_D\begin{bmatrix}\psi_A\\ \psi_B\end{bmatrix}d^3r =\varepsilon'\langle\psi\mid\psi\rangle \tag{A8}$$

and

$$\varepsilon'=\varepsilon+\frac{\int\psi_A^\dagger\frac{\hbar}{4M^2c^2}\sigma\cdot(\nabla V\times\mathbf{p})\psi_A d^3r}{\int(\psi_A^\dagger\psi_A+\psi_B^\dagger\psi_B)d^3r} . \tag{A9}$$

The second term is just the spin-orbit interaction since, for a spherical potential,

$$\nabla V=\frac{1}{r}\frac{dV}{dr}\mathbf{r} \tag{A10}$$

and

$$\mathbf{r}\times\mathbf{p}=\mathbf{L} .$$

Equation (A10) can be rewritten for an arbitrary basis function and is given in Eq. (6). Note that Eq. (6) is written in terms of $\mathbf{s}=\hbar/2\,\sigma$. The importance of this result is that the spin-orbit term is to be evaluated using the large component only. Therefore, in our calculations on solids it is necessary to double the basis set and evaluate Eq. (A9). There are several types of terms because the radial functions are formed from $g(r)$ and the energy derivative $\dot{g}(r)$ and also because the basis functions contain mixtures of different l values.

We also note that the dV/dr form for the spin-orbit interaction follows from the assumed one-electron Dirac Hamiltonian. In reality there are two electron parts, and Blume and Watson[36] have shown that for these dV/dr is not a particularly good approximation. As discussed in Sec. IV C, there is, however, reasonable agreement between the calculated and measured spin-orbit splittings for the valence levels of atoms.

[1]R. Fowler and E. A. Guggenheim, *Statistical Thermodynamics* (Cambridge University Press, London, 1949).
[2]H. Sato and R. S. Toth, Phys. Rev. **124**, 1833 (1961).
[3]R. Kikuchi, in *Noble Metal Alloys*, edited by T. B. Massalski, W. B. Pearson, L. H. Bennett, and Y. A. Chang, (Metallurgical Society, Inc., Warrendale, PA, 1986).
[4]R. C. Kittler and L. M. Falicov, Phys. Rev. B **18**, 2506 (1978); **19**, 291 (1979).

[5]K. Binder, Phys. Rev. Lett. **45**, 811 (1980).
[6]T. M. Buck, G. H. Wheatley, and L. Marchut, Phys. Rev. Lett. **51**, 43 (1983).
[7]E. G. McRae and R. A. Malic, Surf. Sci. **148**, 551 (1984).
[8]R. G. Jordan and G. S. Sohal, J. Phys. C **15**, L663 (1982).
[9]R. G. Jordan, G. S. Sohal, B. L. Gyorffy, P. J. Durham, W. M. Temmerman, and P. Weinberger, J. Phys. F **15**, L135 (1985).
[10]W. Eberhardt, S. C. Wu, R. Garrett, D. Sondericker, and F. Jona, Phys. Rev. B **31**, 8285 (1985).
[11]S. B. DiCenzo, P. H. Citrin, E. H. Hartford, Jr., and G. K. Wertheim, Phys. Rev. B **34**, 1343 (1986).
[12]G. K. Wertheim, Phys. Rev. B **36**, 4432 (1987).
[13]Z. Q. Wang, J. Quinn, C. K. C. Lok, Y. S. Li, F. Jona, and J. W. Davenport (unpublished).
[14]See O. K. Andersen, O. Jepsen, and D. Glötzel, in *Highlights of Condensed-Matter Theory,* edited by F. Bassani, F. Fumi, and M. Tosi (North-Holland, Amsterdam, 1985), p. 59.
[15]K. Terakura, T. Oguchi, T. Mohri, and K. Watanabe, Phys. Rev. B **35**, 2169 (1987).
[16]S.-H. Wei, A. A. Mbaye, L. G. Ferreira, and A. Zunger, Phys. Rev. B **36**, 4163 (1987).
[17]H. L. Skriver and H. P. Lengkeek, Phys. Rev. B **19**, 900 (1979).
[18]J. W. Davenport, Phys. Rev. B **29**, 2896 (1984).
[19]R. E. Watson, J. W. Davenport, and M. Weinert, Phys. Rev. B **35**, 508 (1987).
[20]O. K. Andersen, Phys. Rev. B **12**, 3060 (1975).
[21]R. E. Watson, J. W. Davenport, and M. Weinert, Phys. Rev. B **34**, 8421 (1986).
[22]L. Hedin and B. I. Lundqvist, J. Phys. C **4**, 2064 (1971).
[23]See, e.g., C. T. Chan, D. Vanderbilt, S. G. Louie, and J. R. Chelikowski, Phys. Rev. B **33**, 7941 (1986).
[24]L. F. Mattheiss and D. R. Hamann, Phys. Rev. B **33**, 823 (1986).
[25]J. F. Janak, V. L. Moruzzi, and A. R. Williams, Phys. Rev. B **12**, 1257 (1975).
[26]M. S. S. Brooks and B. Johansson, J. Phys. F **13**, L197 (1983).
[27]R. S. Mulliken, J. Chem. Phys. **23**, 1833 (1955)
[28]A. H. MacDonald, W. E. Pickett, and D. D. Koelling, J. Phys. C **13**, 2675 (1980).
[29]N. E. Christensen and B. O. Seraphin, Phys. Rev. B **4**, 3321 (1971); T. Takeda, J. Phys. F **10**, 1135 (1980).
[30]R. J. Elliott, Phys. Rev. **96**, 280 (1954).
[31]M. Tinkham, *Group Theory and Quantum Mechanics* (McGraw-Hill, New York, 1964), p. 78.
[32]N. E. Christensen, Solid State Commun. **44**, 51 (1982).
[33]M. Weinert, J. W. Davenport, and R. E. Watson, Phys. Rev. B **34**, 2971 (1986).
[34]R. E. Watson, J. Hudis, and M. L. Perlman, Phys. Rev. B **4**, 4139 (1974).
[35]D. D. Koelling and B. N. Harmon, J. Phys. C **10**, 3107 (1977).
[36]M. Blume and R. E. Watson, Proc. R. Soc. London, Ser. A **270**, 127 (1962).